

TORCH: Time of Flight Identification with Cherenkov Radiation

M. J. Charles^a, R. Forty^b, on behalf of the LHCb Collaboration

^a*Department of Physics, University of Oxford, Oxford, United Kingdom.*

^b*European Organisation for Nuclear Research (CERN), Geneva, Switzerland.*

Abstract

TORCH is a time-of-flight detector concept using Cherenkov light to provide charged particle identification up to 10 GeV/c. The concept and design are described and performance in simulation is quantified.

Keywords: Cherenkov, particle identification

1. Introduction

Charged particle identification is critical for a heavy flavour physics experiment. It is required both for separating signal decays from more copious backgrounds, such as $B_s^0 \rightarrow D_s^- K^+$ from $B_s^0 \rightarrow D_s^- \pi^+$, and for tagging the initial flavour of neutral mesons which may undergo mixing. One way to accomplish this is with a Ring Imaging Cherenkov (RICH) system, in which mass hypotheses are tested by measuring the angle (θ_C) and number of Cherenkov photons emitted by a charged particle passing through a radiator. For a given detector geometry, the separation power between K and π hypotheses depends on the refractive index n of the radiator and the momentum p of the particle. Between the pion and kaon thresholds, pions are positively identified but kaons are identified only by the absence of photons. In principle this can provide good separation, but it is vulnerable to background from fake tracks (e.g. due to mistakes in pattern recognition in the tracking system), which cannot create Cherenkov photons and so would be identified as kaons. Likewise, protons would not be distinguished from kaons. Therefore, it is desirable to work above the kaon threshold—and in an environment with high occupancy in the tracking system or a large number of protons, it is essential.

At LHCb [1], particle identification is needed for the momentum range from 2 GeV/c to 100 GeV/c. This is currently accomplished by a RICH system [2] consisting of two detectors with three radiators. Two of these are gaseous: C₄F₁₀ and CF₄,

with refractive indices of 1.0014 and 1.0005, respectively, for visible light at STP. These correspond to kaon Cherenkov thresholds of 9.3 and 15.6 GeV/c, and together provide better than 3σ kaon-pion separation up to 100 GeV/c. Positive kaon identification from 2–10 GeV/c requires a third radiator with a kaon Cherenkov threshold around 2 GeV/c, corresponding to $n \approx 1.03$. This excludes conventional materials: the phase transition from gas to liquid or solid is associated with a large jump in $(n-1)$ from $\mathcal{O}(10^{-3})$ or smaller to $\mathcal{O}(1)$. The low density of aerogel gives it a suitable refractive index: LHCb's third radiator is aerogel with $n = 1.029$ in air and $n = 1.037$ in C₄F₁₀. However, Rayleigh scattering limits the useful light yield: approximately 7 detected photoelectrons are expected at LHCb for a saturated track in aerogel. In a high-background scenario, such as the proposed LHCb upgrade from $2 \times 10^{32} \text{ cm}^{-2} \text{ s}^{-1}$ to $2 \times 10^{33} \text{ cm}^{-2} \text{ s}^{-1}$, kaon-pion discrimination from aerogel would be severely compromised [3].

Another method of charged particle identification is by time of flight measurement. The principle is simple: if a particle of mass m is detected at position x and time t after leaving the origin, then

$$t = \frac{x}{c} \sqrt{1 + \left(\frac{m}{p}\right)^2} \approx \frac{x}{c} \left[1 + \frac{1}{2} \left(\frac{m}{p}\right)^2\right] \quad (1)$$

and so the difference in expected time between kaons and pions would be

$$t_K - t_\pi \approx \frac{x}{c} \frac{1}{2p^2} [m_K^2 - m_\pi^2]. \quad (2)$$

Therefore, to obtain 3σ separation between the two hypotheses the time resolution σ_t must satisfy

$$\sigma_t < \frac{1}{3} \frac{x}{c} \frac{1}{2p^2} [m_K^2 - m_\pi^2]. \quad (3)$$

If this approach were to be used for kaon identification in the range 2–10 GeV/ c and the path length were $x = 10$ m, then a per-track time resolution $\sigma_t < 12.5$ ps would be required. A very fast response would be needed—Cherenkov radiation would be suitable for this purpose. If the expected light yield were 50 detected photoelectrons, a per-photon time resolution under 90 ps would be required.

A third method is to measure the time of propagation τ_γ over a path length d_γ of Cherenkov photons emitted by a charged particle. In a dispersive medium, photons propagate at the group velocity c/n_g , and so

$$n_g = c \frac{\tau_\gamma}{d_\gamma}. \quad (4)$$

The relationship between n and n_g is a non-linear function that depends on the medium but obeys:

$$n_g = n - \lambda \frac{dn}{d\lambda}. \quad (5)$$

After computing n from n_g , the mass of the particle can be extracted:

$$\beta = \frac{1}{n \cos \theta_C} \quad (6)$$

$$\Rightarrow m = p \sqrt{n^2 \cos^2 \theta_C - 1}. \quad (7)$$

The methods outlined above may be combined in an elegant way. Consider a large, thin plane of an optically dense medium such as quartz. Charged particles passing through the plane emit Cherenkov photons, which propagate to the edges via total internal reflection as in the BABAR DIRC [4]. The arrival time of a photon at the edge of the plane is the sum of the time of flight of the track to the emission point, t , and the time of propagation of the photon in the medium, τ_γ . Then

$$t + \tau_\gamma = \frac{x}{c} \sqrt{1 + \left(\frac{m}{p}\right)^2} + \frac{d_\gamma n_g}{c} \quad (8)$$

where n_g may be determined from

$$n = \frac{1}{\beta \cos \theta_C} = \frac{\sqrt{m^2 + p^2}}{p \cos \theta_C}. \quad (9)$$

Both dt/dm and $d\tau_\gamma/dm$ have the same sign so the two effects combine constructively. For a given track, the first term of Eq. 8 is fixed but the second depends on the direction and path length of the photon, which must be reconstructed for each photon individually—for the planar geometry outlined above, this can be done by measuring two independent angles for each photon. This is the principle behind the design of the TORCH, and of the Belle upgrade TOP [5] and PANDA endcap DIRC [6] which inspired it.

2. TORCH design

The TORCH detector consists of a plane of quartz covering the full LHCb angular acceptance and placed 12 m downstream of the interaction point, plus focusing elements and photodetectors along each edge. The quartz plate has dimensions 7440 mm \times 6120 mm, with a hole of 26 mm \times 26 mm at the centre for the beam pipe, as illustrated in Fig. 1. The focusing element uses a cylindrical mirror to focus the light such that the distance along the photodetector plane is approximately proportional to the angle θ_z , as illustrated in Fig. 2. This angle is key: the overall resolution is dominated by the pixelization uncertainty on θ_z . From simulation studies, we find that a 128-channel segmentation and a dynamic range of 400 mrad corresponds to an uncertainty of 0.96 mrad on θ_z and per-photon uncertainty on the time of propagation of $\mathcal{O}(70)$ ps. The granularity requirement in the other dimension is much looser, since the azimuthal angle is typically measured with a lever arm of a few metres: $\mathcal{O}(1)$ cm is sufficient match the 1 mrad resolution.

The key property required of the photodetector is high speed: its intrinsic time spread should be significantly better than 90 ps. The photon detection technology which currently gives the best time resolution is the use of micro-channel plate photomultipliers (MCP-PMT). They have been used in R&D for a related concept under development by the Belle collaboration for their upgrade [7], with single-photon time resolutions of 35 ps achieved.

An example of a commercially-available detector of this type which comes close to satisfying the requirements of TORCH is the PhotonisTM XP85022 MCP-PMT. This is available in a 1024-channel version, with an array of 32 \times 32 pixels in a 53 \times 53 mm² active area, and overall dimension of 59 mm. For the sake of developing a concrete design for TORCH we have assumed the use of this photodetector, laid

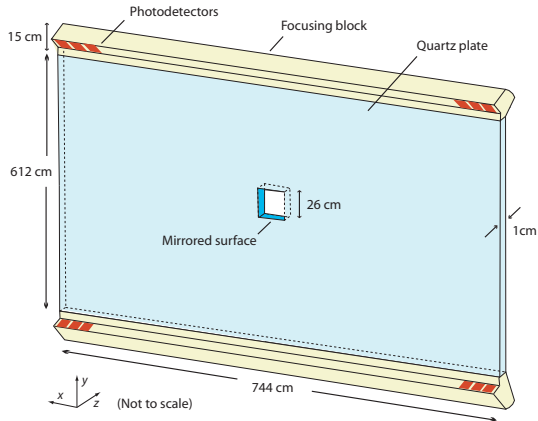


Figure 1: Schematic layout of the TORCH detector. For clarity, focusing elements have only been shown on the upper and lower edges. Photodetectors extend along the full length of each edge.

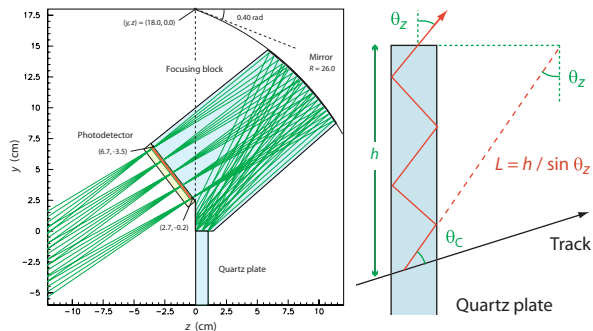


Figure 2: Cross section of the focusing element (left), and definition of the angle θ_z (right). The focusing of photons is shown for five illustrative angles between 450 and 850 mrad, emerging at different points across the edge of the plate.

side-by-side with a pitch of 60 mm along the edges of the plane. The anode structure of an MCP-PMT consists simply of conductive pads to read out the charge, and the pixellization can therefore in principle be adjusted. For the simulation of TORCH we have assumed an array of 8×128 pixels of dimension $6.6 \text{ mm} \times 0.4 \text{ mm}$.

3. Reconstruction and pattern recognition

Following the approach outlined in Sec. 1 for the design from Sec. 2, the reconstruction is relatively straightforward: we measure the arrival time and position of a photon on the photodetector plane, infer θ_z , and calculate its trajectory assuming it was emitted by the track at the midpoint in z of its path

through the quartz block. Given measurements of the track path and momentum from a tracking system and knowledge of the optical properties of quartz, this is sufficient information to compute all quantities in Eq. 8 and 9 and extract the mass from $t + \tau_\gamma$. There are two major practical challenges, though: first, association of photons to tracks (pattern recognition); and second, determining the time when the track left the origin.

Pattern recognition is critical: in the environment of the upgraded LHCb luminosity, there may be $\mathcal{O}(100)$ fully reconstructed tracks plus a large number of secondaries passing through the TORCH in an event. However, most photon-track pairs can be rejected as unphysical. We take advantage of the limited range of photon wavelengths to which the photodetector is sensitive and reject candidates outside this range. This is mathematically equivalent to a restriction on θ_C : for our geometry, this means that relevant photons lie roughly along arcs on the photodetector plane. Additionally, we can ignore photon-track pairs with unphysical timing. Instead of attempting to measure the mass of the particle directly, we assume e, μ, π, K, p hypotheses and test for consistency with each in turn. Background photons whose timing is not consistent with any of these masses can be ignored.

In Sec. 1 it was assumed that the track left the origin at $t = 0$ —or equivalently, that the relative timing between the photodetector and the initial collision is known. However, we cannot rely on an external clock for 10 ps-level timing—and even if we could, the luminous region at LHCb extends a few cm in z , which would add a smearing of order a few tens of ps. We must therefore measure the track start time ourselves. One approach would be to install a second TORCH-like detector close to the interaction point, at the price of additional cost, material, and time resolution. A more efficient solution is to take advantage of the high pion multiplicity at a hadron collider and use other tracks from the same event primary vertex to fix the relative timing. The same reconstruction procedure described above is used except that the last step is inverted: for each track from the event primary vertex, the pion mass is assumed as the input and the time elapsed ($t + \tau_\gamma$) is calculated from Eq. 8. Subtracting this from the measured photon detection time gives a measurement of the track start time. For a primary vertex with N_π fully reconstructed pion tracks, the start time resolution is smaller than the per-track time resolution by roughly $\sqrt{N_\pi}$.

4. Performance

To test the particle identification performance, we take events from the full LHCb Monte Carlo simulation, determine the set of charged particles that would pass through the TORCH, simulate the emission, propagation, and detection of Cherenkov radiation in the TORCH for these particles with a stand-alone program, then apply the reconstruction and pattern-recognition procedure outlined above to the output. No truth information is used for the reconstruction and pattern-recognition. However, a number of simplifying assumptions were made: perfect measurements of track position and momentum, perfect extrapolation of tracks through the magnetic field of the detector, negligible electronics noise and cross-talk; negligible spill-over between events; and no multiple scattering, delta ray emission, or inelastic collisions in the TORCH. Background from certain sources such as backscatter from the calorimeters was not available to the simulation and was also neglected.

We characterize the performance in terms of particle identification efficiencies for those kaon and pion tracks which would be useful for physics analysis. Specifically, we require tracks to be well-measured (with track segments found both upstream and downstream of the magnet), well-matched to an event primary vertex, and associated to a kaon or pion in the Monte Carlo truth information. Tracks are identified either as kaons or as pions according to which of the two hypotheses is found to be most consistent by the pattern recognition. The efficiency is shown as a function of track momentum in Fig. 3 for events simulated at a luminosity of $L = 2 \times 10^{32} \text{ cm}^{-2} \text{ s}^{-1}$. The efficiency for correct identification is $> 95\%$ up to $10 \text{ GeV}/c$, dropping at higher momentum as the time difference between kaon and pion hypotheses diminishes.

5. Conclusions

The TORCH concept is intended to provide charged particle identification in the momentum range $2\text{--}10 \text{ GeV}/c$ in a high-rate environment. It has been shown that the pattern-recognition problem is solvable and that target performance can be reached under simplified conditions. The challenge is now to test whether this performance can be maintained under realistic conditions and at $L = 2 \times 10^{33} \text{ cm}^{-2} \text{ s}^{-1}$. This will require prototype tests and more detailed simulation. A revised,

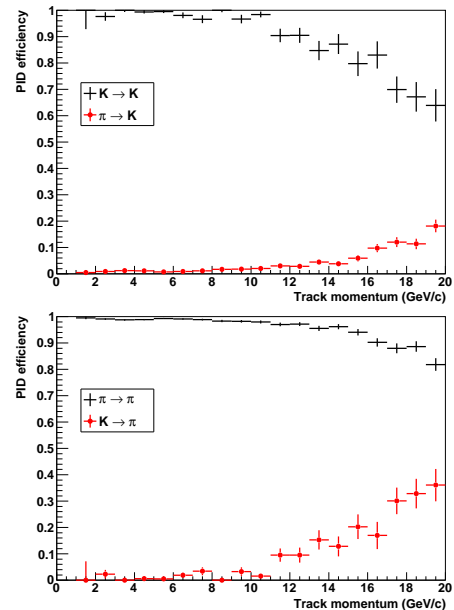


Figure 3: Identification efficiency of the subset of well-measured charged tracks which are well-matched to a primary vertex. The plots show the efficiency for a kaon (upper) or pion (lower) track to be identified correctly (black) or incorrectly (red/dot), considering only the kaon and pion hypotheses.

modular design with a smaller quartz plane is also under investigation.

6. Acknowledgements

The TORCH concept has evolved from ideas that have been demonstrated in the BABAR DIRC, and related developments that are under study by the PANDA and Belle collaborations. It is a pleasure to thank Bjoern Seitz for fruitful discussion, and our colleagues in the LHCb RICH group for their interest.

References

- [1] LHCb Collaboration, A. A. Alves *et al.*, JINST **3** (2008) S08005.
- [2] LHCb collaboration, S. Amato *et al.*, CERN-LHCC-2000-037.
- [3] Y. M. Kim, these proceedings.
- [4] BABAR Collaboration, B. Aubert *et al.*, Nucl. Instrum. Methods Phys. Res., Sect. A **479** (2002) 1.
- [5] M. Akatsu *et al.*, Nucl. Instrum. Meth. A **440** (2000) 124.
- [6] K. Fohl *et al.*, Nucl. Instrum. Meth. A **595** (2008) 88.
- [7] K. Inami, Nucl. Instrum. Meth. A **595** (2008) 96.